

Title	Properties of Particle Scattering Functions for Two Types of Spherical Micelles Composed of Hard Core and Shell of Symmetrically Arranged Rods or Shell of Gaussian Subchains (Commemoration Issue Dedicated to Professor Hiroshi Ibagaki, Professor Michio Kurata, Professor Ryozo Kitamura, On the Occasion of Their Retirements)
Author(s)	Tsunashima, Yoshisuke; Hirata, Masukazu; Kurata, Michio
Citation	Bulletin of the Institute for Chemical Research, Kyoto University (1989), 66(3): 184-193
Issue Date	1989-02-15
URL	http://hdl.handle.net/2433/77243
Right	
Type	Departmental Bulletin Paper
Textversion	publisher

Properties of Particle Scattering Functions for Two Types of Spherical Micelles Composed of Hard Core and Shell of Symmetrically Arranged Rods or Shell of Gaussian Subchains

Yoshisuke TSUNASHIMA, Masukazu HIRATA, and Michio KURATA*

Received September 9, 1988

The particle scattering function $P(q)$ and the apparent mean-square radius of gyration $\langle S^2 \rangle_{app}$ were examined theoretically for two types of micelles which are composed of "two-phases"; the hard core and the shell of symmetrically arranged rods or the shell of Gaussian subchains. In this examination, the parameters concerning the micellar structures and the optical densities of the phases were varied in the wide range and the behavior of $P(q)$ and $\langle S^2 \rangle_{app}$ for the two micelles was compared in detail. $P(q)$ showed the oscillatory feature for both micelles but the feature was much remarkable for the rodlike-shell micelles. $\langle S^2 \rangle_{app}$ decreased linearly from positive to negative values with increasing the weight-fraction refractive index increment of the core y for the rodlike-shell micelles and for the Gaussian-shell micelles of infinite number of association. In the case of finite association of the molecules, $\langle S^2 \rangle_{app}$ became a quadratic form of y . Moreover, it was found that the behavior predicted for the rodlike-shell micelles explained well the experimental data which was obtained for the ionic-non-ionic diblock copolymer in aqueous solution.

KEY WORDS: Particle Scattering Function/ Mean-Square radius of Gyration/ Micelles/ Diblock Copolymers/

INTRODUCTION

Block copolymers form in dilute solution, especially of selective solvents, various types of micellar structures due to the microphase separation of the constituent subchains. The chemical species and composition of the polymers are one of the basic factors which control the types of the structure formed. The structure of AB diblock copolymers in very dilute solution can simply be represented by the models of the "two-phase" spherical multimolecular micelles which are composed of a pure B phase constructing the spherical "inner core" and a pure A phase constructing the "outer shell". The shell phase has been treated theoretically by Tanaka et al. with the random-flight chains^{1,2} or by Hirata and Tsunashima with the rods arranged symmetrically around the core³ under the assumption that thermodynamic interactions between chemically different A and B monomers are not taken into account. The former is comparable to the micelles formed by *non-ionic* block copolymers in *organic* solvents selective for A chains,² while the latter to the micelles formed by *ionic-non-ionic* block copolymers in *aqueous* solution. The two types of models¹⁻³ show the interesting feature in the particle scattering function and the mean-square (ms) radius of gyration which are characteristic of their own structures. In this paper, this feature is compared

* 網島良祐, 平田益一, 倉田道夫: Laboratory of Fundamental Materials Properties, Institute for Chemical Research, Kyoto University Uji, Kyoto 611.

in detail to each other over the wide range of the parameters controlling both the micellar structures and the optical density of subchains in given solvents. It is then made clear that the differences appeared in the particle scattering function and ms radius of gyration for the two models are caused by the highly symmetrical arrangement of rods in the rodlike-shell model. Finally it is shown that the model of the rodlike-shell micelles expresses satisfactorily the static light scattering data which has been obtained for an ionic-non-ionic diblock copolymer, poly(N-ethyl-2-vinylpyridinium hydroxide)-*block*-polystyrene in extremely dilute salt-free aqueous solution.⁴

OUTLINE OF PARTICLE SCATTERING FUNCTION AND MEAN-SQUARE RADIUS OF GYRATION FOR TWO TYPES OF MICELLES

Let w_t and ν_t be the weight fraction and refractive index increment of the inner core ($t=i$) and the outer shell ($t=o$) for a micelle, respectively. The particle scattering function $p(q)$ and the apparent ms radius of gyration $\langle S^2 \rangle_{app}$ of the micelle considered here are then be expressed by^{5,6}

$$\begin{aligned} P(q) &= y^2 P_i(q) + (1-y)^2 P_o(q) + 2y(1-y) P_{io}(q) \\ \langle S^2 \rangle_{app} &= y^2 \langle S^2 \rangle_i + (1-y)^2 \langle S^2 \rangle_o + 2y(1-y) \langle S^2 \rangle_{io} \end{aligned} \quad (1)$$

with y the weight-fraction refractive index increment of the core part

$$y = w_i \nu_i / (w_i \nu_i + w_o \nu_o) \quad (2)$$

Here the quantities $P_t(q)$ or $\langle S^2 \rangle_t$ with subscript $t=i, o,$ and io represent the values corresponding to the inner core, the outer shell, and the interference between the core and the shell, respectively. The shell has n rays of rods of length L for the rodlike-shell micelles or n rays of Gaussian chains of ms radius of gyration $\langle S^2 \rangle_{SG}$ for the Gaussian-shell micelles. The core is a rigid sphere of radius r_c in both micelles. With these structure parameters $n, r_c, L,$ or $\langle S^2 \rangle_{SG},$ the quantities P_t and $\langle S^2 \rangle_t$ for both micelles have been formulated as described below.

Particle Scattering Function

$P_i(q)$ has the form for a hard sphere which was obtained long ago⁷

$$P_i(q) = (3/x^3)^2 (\sin x - x \cos x)^2, \quad x = qr_c \quad (3)$$

where q is the magnitude of the scattering vector and is defined as $q = (4\pi n_0 / \lambda_0) \sin(\theta/2)$ with n_0 the refractive index of the solvent, λ_0 the wavelength of the incident light in vacuum, and θ the scattering angle.

For the rodlike-shell micelles, it becomes that³

$$P_o(q) = n^{-2} \sum_{t=0}^d c_t P_o(q, \theta_t) \quad (4)$$

$$\begin{aligned} P_o(q, \theta_t) &= \int_0^1 \int_0^1 \{ \sin [qLr(s_j, s_k, \theta_t)] / qLr(s_j, s_k, \theta_t) \} ds_j ds_k \\ r(s_j, s_k, \theta_t) &= [(s_j + r_c/L)^2 + (s_k + r_c/L)^2 - 2(s_j + r_c/L)(s_k + r_c/L) \cos \theta_t]^{1/2} \end{aligned}$$

$$P_{io}(q) = (3/2)(r_c/L)^{-3} \int_0^1 \int_0^\pi \int_0^{r_c/L} \{ \sin [qLr(s, u, \theta)] / qLr(s, u, \theta) \} u^2 \times \sin \theta \, du \, d\theta \, ds \quad (5)$$

$$r(s, u, \theta) = [u^2 + (s + r_c/L)^2 - 2u(s + r_c/L)\cos \theta]^{1/2}$$

with $\sum_{t=1}^d c_t = n(n-1)$. Eq 4 shows that $P_o(q)$ is the sum of the *partial* particle scattering functions $P_o(q, \theta_t)$ for the intra-rod interference ($t=\text{zero}$ with $c_t=n$ and $\theta_t=0$) and the inter-rod interferences ($t=1 \sim d$). The latter depends strongly on the spatial symmetry of a pair of rods which are arranged in space at an angle θ_t . $Lr(s_j, s_k, \theta_t)$ is a distance between the j th and k th segments at the positions s_j and s_k on the two rods. Thus $P_o(q)$ becomes a function of n and r_c/L . While $P_{io}(q)$ is a function of r_c/L and is independent of n . Hirata and Tsunashima³ have selected a series of n values, i.e., $n=3, 4, 6, 8, 12, 20, 32$, and 92 , with which the rods can be arranged symmetrically in space. For these n , the evaluation of the integrals in eqs 4 and 5 have been made numerically on FACOM M-380Q computer and the values of $P_o(q)$ and $P_{io}(q)$ have been tabulated as a function of r_c/L .

For the Gaussian-shell micelles, $P_o(q)$ becomes the sum of Debye function for a single Gaussian chain $P_{o1}(q)$ and the interchain interference $P_{o2}(q)$:^{1,2}

$$P_o(q) = (1/n)P_{o1}(q) + (1 - 1/n)P_{o2}(q) \quad (6)$$

$$P_{o1}(q) = (2/x^2) [\exp(-x) - 1 + x], \quad x = q^2 \langle S^2 \rangle_{SG} = (1/4)(qD)^2$$

$$P_{o2}^{1/2}(q) = 4(1 + 2r_c/D \pi^{1/2})^{-1} \int_{r_c/D}^{\infty} \{ r[1 - \text{erf}(r - r_c/D)] - (r_c/D) \times [1 - \text{erf}(2r - 2r_c/D)] \} \{ \sin(qDr) / qDr \} dr$$

Here r denotes the radial distance of a segment in the Gaussian chain and is reduced by the chain diameter $D \equiv 2 \langle S^2 \rangle_{SG}^{1/2}$. Tanaka et al.^{1,2} have pursued the integral in $P_{o2}(q)$ by using Monte Carlo method. However, we approximated it by the integration over the range from r_c/D to $r_c/D + 6$ because the value concerning the error function $1 - \text{erf}(5)$ is less than 10^{-10} . The $P_o(q)$ thus estimated is a function of n and r_c/D . On the other hand, the interference term between the core and the shell is a function of a single parameter r_c/D :

$$P_{io}(q) = [P_i(q)P_{o2}(q)]^{1/2} = (3/x^3)(\sin x - x \cos x)P_{o2}^{1/2}(q), \quad x = qr_c \quad (7)$$

Mean-Square Radius of Gyration

For the rodlike shell model, $\langle S^2 \rangle_o$ becomes independent of n because of the highly symmetrical arrangement of rods. $\langle S^2 \rangle_{app}$ then comes into a simple form³ which is expressed by a linear function of y as

$$\langle S^2 \rangle_{app} / L^2 = [(r_c/L)^2 + (r_c/L) + 1/3] - [(2/5)(r_c/L)^2 + (r_c/L) + 1/3]y \quad (8)$$

where we used the relation $2 \langle S^2 \rangle_{io} = \langle S^2 \rangle_i + \langle S^2 \rangle_o$.

For the Gaussian-shell model, $\langle S^2 \rangle_o$ is the sum of the intrachain dimension

Micelles Composed of Hard Core and Rodlike Shell or Gaussian Shell

$\langle S^2 \rangle_{o1}$ and the interchain dimension $\langle S^2 \rangle_{o2}$,

$$\langle S^2 \rangle_o = (1/n)\langle S^2 \rangle_{o1} + (1-1/n)\langle S^2 \rangle_{o2} \quad (9)$$

$$\langle S^2 \rangle_{o1} = \langle S^2 \rangle_{SG}$$

$$\langle S^2 \rangle_{o2} = \left\{ (3/4) + (r_c/D)^2 + (7/3\pi^{1/2})(r_c/D) \right. \\ \left. \times [1 + (9\pi^{1/2}/14)(r_c/D)] / [1 + (2/\pi^{1/2})(r_c/D)] \right\} 4\langle S^2 \rangle_{SG}$$

The interference term $\langle S^2 \rangle_{io}$ becomes

$$\langle S^2 \rangle_{io} = (\langle S^2 \rangle_i + \langle S^2 \rangle_{o2})/2 \quad (10)$$

with $\langle S^2 \rangle_i = (3/5)r_c^2$. The low spatial symmetry of the Gaussian chains gives n dependence in $\langle S^2 \rangle_o$ and brings $\langle S^2 \rangle_{app}$ into a quadratic form of y

$$\langle S^2 \rangle_{app} = \langle S^2 \rangle_{o2} - (1/n)(1+y^2)\langle S^2 \rangle_{12} \\ + y[(\langle S^2 \rangle_i - \langle S^2 \rangle_{o2}) + (2/n)\langle S^2 \rangle_{12}] \quad (11)$$

$$\langle S^2 \rangle_{12} = \langle S^2 \rangle_{o2} - \langle S^2 \rangle_{o1}$$

At $n \rightarrow \infty$, $\langle S^2 \rangle_{app}$ becomes a linear function of y , which is similar to eq 8

$$\langle S^2 \rangle_{app} = \langle S^2 \rangle_{o2} + (\langle S^2 \rangle_i - \langle S^2 \rangle_{o2})y \quad (n \rightarrow \infty) \quad (12)$$

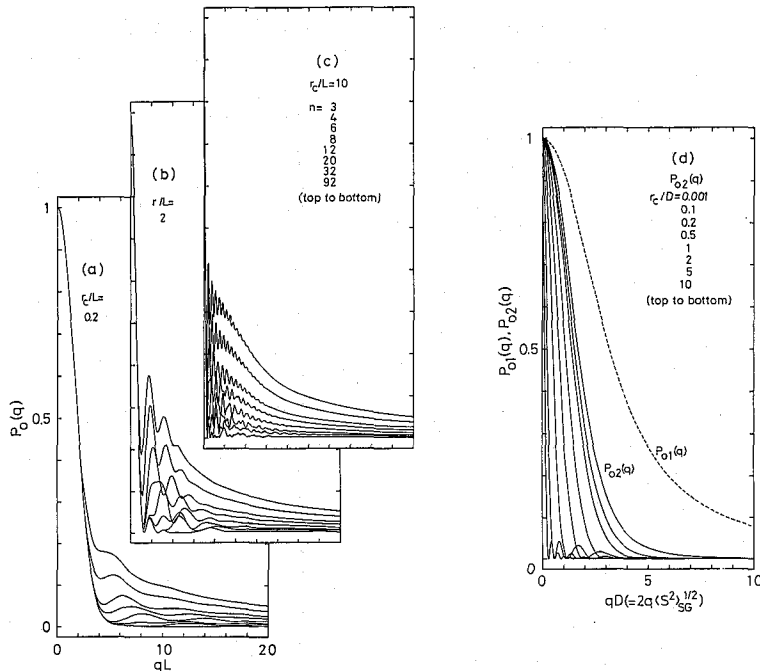


Figure 1(a)-(d). The particle scattering functions for the rodlike shell $P_o(q)$ with (a) $r_c/L=0.2$, (b) $r_c/L=2$, and (c) $r_c/L=10$. The number of rods n is changed as 3, 4, 6, 8, 12, 20, 32, and 92 from the top to the bottom. (d) The particle scattering functions for the shell of Gaussian chains. The broken line represents the intrachain part $P_{o1}(q)$ and the solid lines represent the interchain part $P_{o2}(q)$, the ratio $r_c/2\langle S^2 \rangle_{SG}^{1/2}$ being 0.001, 0.1, 0.2, 0.5, 1, 2, 5, and 10 from the top to the bottom.

PROPERTIES OF PARTICLE SCATTERING FUNCTIONS FOR MICELLES

The particle scattering functions for the rodlike shell part $P_o(q)$ are illustrated in Figure 1(a), (b), and (c) as a function of qL for $r_c/L=0.2, 2, \text{ and } 10$, respectively. The number of rods or the association number in the micelles n is changed from 3 to 92 in each figure. These functions for each n , which correspond to the hollow micelles of n rods, come to show many oscillatory peaks as r_c/L increases. This indicates that at a constant length of the rod, the rod-rod interference effect on $P_o(q)$ becomes stronger as the distance between pairs of rods is spread wider due to the increase of the core size. This feature contrasts well with the feature observed for the Gaussian shell, which is shown in Figure 1(d). Here the broken curve represents the qD dependence of $P_{o1}(q)$ ⁸ and the solid curves represent those of $P_{o2}(q)$ at different values of r_c/D . The $P_{o2}(q)$ shows the oscillatory forms at larger r_c/D but the peak heights are lower than those for the rodlike shell. Since $P_o(q)$ is given by summation of P_{o1} and P_{o2} terms (eq 6), the peaks appeared in P_o for the Gaussian shell are small and only a few of them can be detectable. The reason is that in the Gaussian shell, the spatial positions of a pair of chain segments are determined by a probability density,^{1,2} not by a rigid symmetrical rule which is realized in the rodlike shell.

Figure 2(a) and (b) show the interference terms between the core and the shell $P_{io}(q)$ for the rodlike- and Gaussian-shell models, respectively, as a function of qL or qD . When the core size is relatively small as compared with the shell size, i.e., $0 < r_c/L$ (or r_c/D) ≤ 0.2 , $P_{io}(q)$ for both types of models are different much in the shapes each

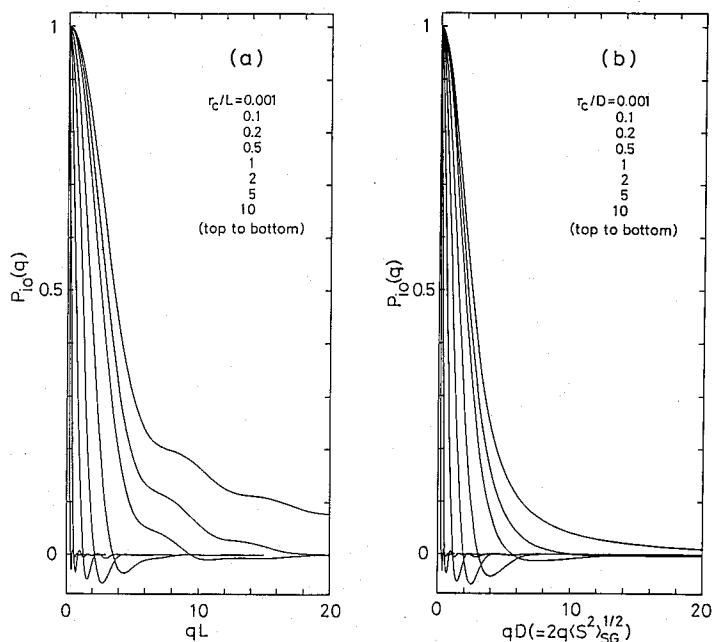


Figure 2. The particle scattering functions due to the interference between the core and the shell $P_{io}(q)$: (a) the shell is rods; (b) the shell is Gaussian chains. r_c/L or $r_c/2 \langle S^2 \rangle_{SG}^{1/2}$ is 0.001, 0.1, 0.2, 0.5, 1, 2, 5, and 10 from the top to the bottom.

other. The oscillatory damping feature (shoulders) observed only for the rodlike-shell model at $r_c/L=0.001, 0.1,$ and 0.2 are caused by the *long* rod arranged around the *small* size of the core. At larger r_c/L , however, the differences in $P_{io}(q)$ are little and the common features are observed which are arized from the interferences between the smaller length of the shell and the larger size of the core.

The particle scattering function of micelles $P(q)$ is evaluated from eq 1. The results for $n=6$ and 32 are illustrated in Figure 3-5 in the form of Kratky plot, i.e., $(qL)^2P$ vs qL or $(qD)^2P$ vs qD plot. Here $P(q)$ is shown at $y>0$ and $y<0$, separately, for three cases of $r_c/L=0.1, 1,$ and 10 . In the figures the solid curves represent the rodlike-shell micelles and the broken curves represent the Gaussian-shell micelles. In the small region of qL or qD (hereafter abbreviated as $qL(D)$), say less than 2, the rodlike-shell micelles show one or a few peaks in $(qL(D))^2P(q)$ at $y\leq 0$, irrespective of the $r_c/L(D)$ values, and reveal remarkable difference in behavior from the Gaussian-shell micelles. The difference is clear at $n=6$ but becomes obscure with increase of n , e.g., at $n=32$. This feature will be visualized later in the dependences of $\langle S^2 \rangle_{app}$ on n and on $r_c/L(D)$ at $y\leq 0$, since $\langle S^2 \rangle_{app}$ is determined by the initial slope of the $P(q)$. On the other hand, such a difference can never be observed at $y>0$; $(qL(D))^2P$ for both micelles resemble each other in behavior.

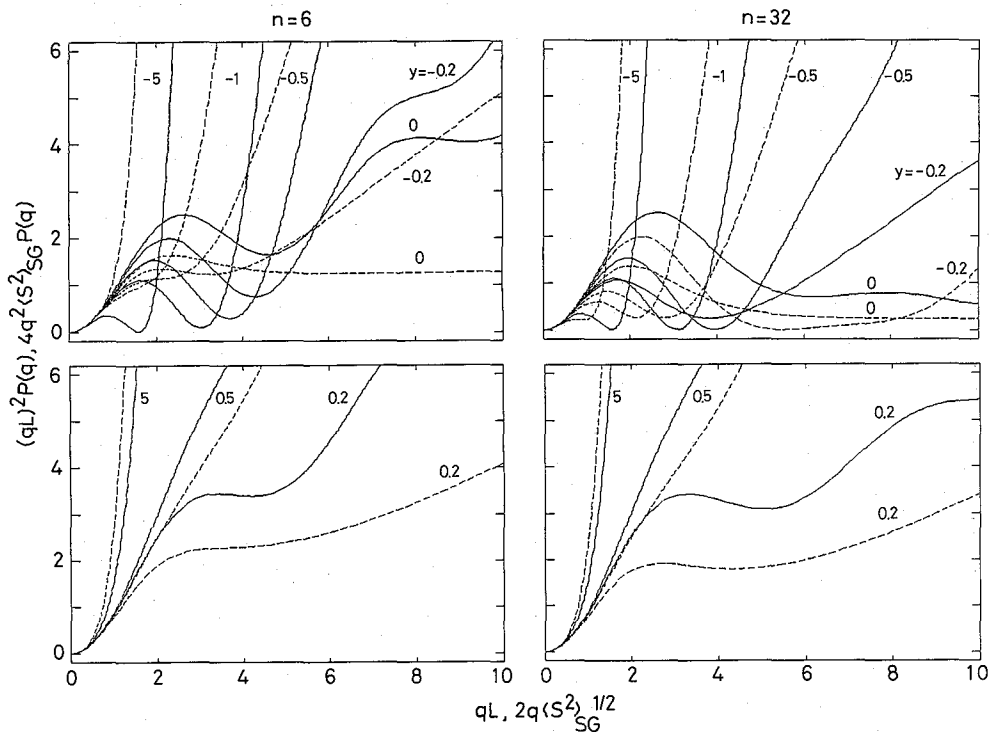


Figure 3. The Kratky plots of the particle scattering functions for the rodlike-shell and the Gaussian-shell micelles $P(q)$ at r_c/L and $r_c/2\langle S^2 \rangle_{SG}^{1/2}=0.1$, respectively. The solid lines represent the former and the broken lines the latter. Two cases that $n=6$ and 32 are shown by changing the parameter y discretely from -5 to 5 .

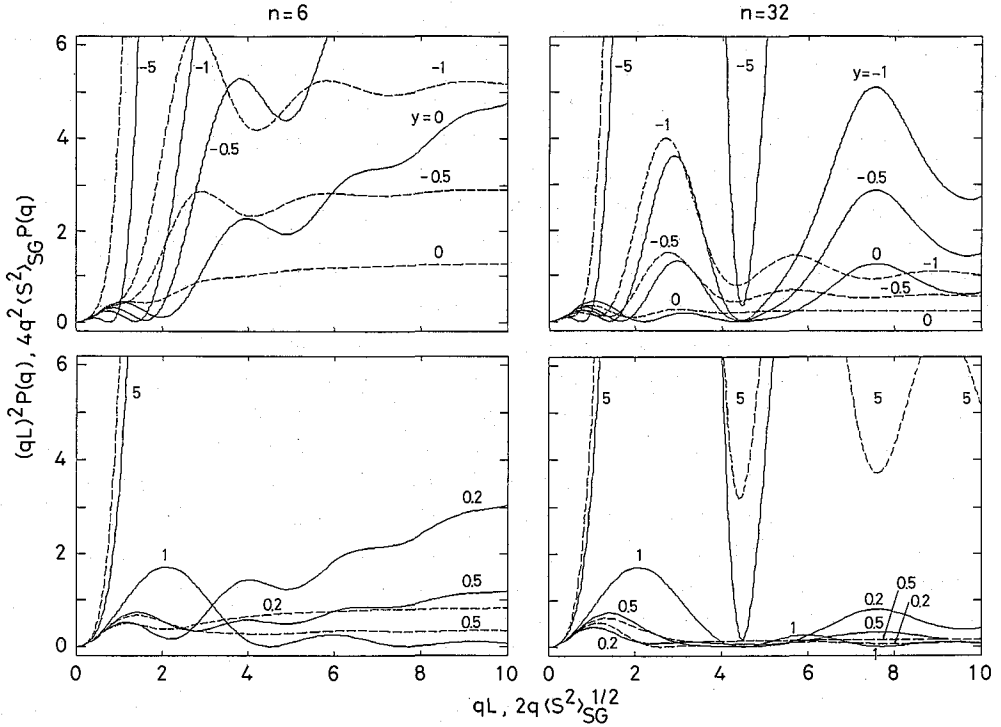


Figure 4. The same plots as in Figure 3 but at r_c/L or $r_c/2\langle S^2 \rangle_{SG}^{1/2} = 1$.

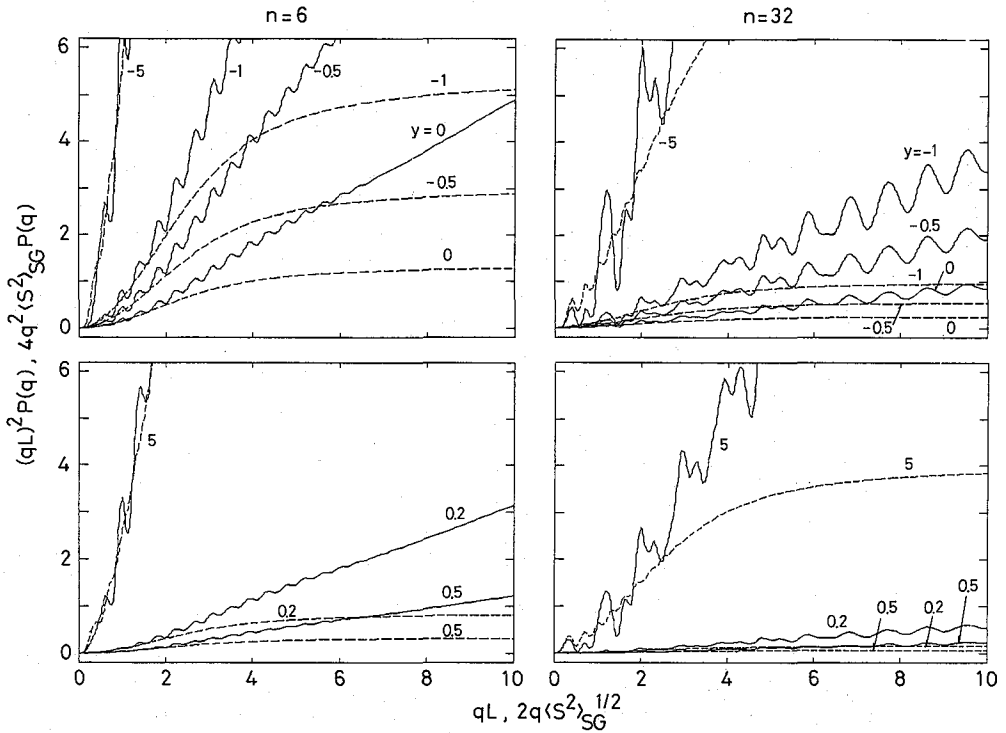


Figure 5. The same plots as in Figure 3 but at r_c/L or $r_c/2\langle S^2 \rangle_{SG}^{1/2} = 10$.

In the larger region of $qL(D)$, the damped oscillatory peaks appear in $P(q)$ for the rodlike-shell micelles, irrespective of the sign in y . The oscillatory feature becomes strong as the $r_c/L(D)$ value increases. The feature also continues up to larger $qL(D)$ region when the value of n is so large as $n=32$. Contrary, the Gaussian-shell micelles do not clearly show such an oscillatory feature in this $qL(D)$ region, and especially never at $qL(D) > 6$. It is already shown in Figure 2 that $P_{io}(q)$ is different around $qL(D) > 6$ for the two micelles with $r_c/L(D) \leq 0.2$. The influence of this difference on $P(q)$ is, however, screened by the more effective $P_o(q)$ term and can not be detected on the $(qL(D))^2 P$ curves for $r_c/L = 0.1$ at $qL(D) > 6$ (Figure 3). Thus the distinct difference in $P(q)$ between the two types of micelles are caused mainly by the $P_o(q)$ structures which are determined by the characteristics of the shell.

PROPERTIES OF MEAN-SQUARE RADIUS OF GYRATION OF MICELLES

The behavior of $\langle S^2 \rangle_{app}$ for two micelles is illustrated in Figure 6. Here the reduced values $\langle S^2 \rangle_{app}/4\langle S^2 \rangle_{SG}$ at $n=10, 50$, and ∞ for the Gaussian-shell micelles and $\langle S^2 \rangle_{app}/L^2$ for the rodlike-shell micelles are plotted against y . The parameters are r_c/D and r_c/L , respectively. At finite n , the $\langle S^2 \rangle_{app}$ for Gaussian-shell micelles is

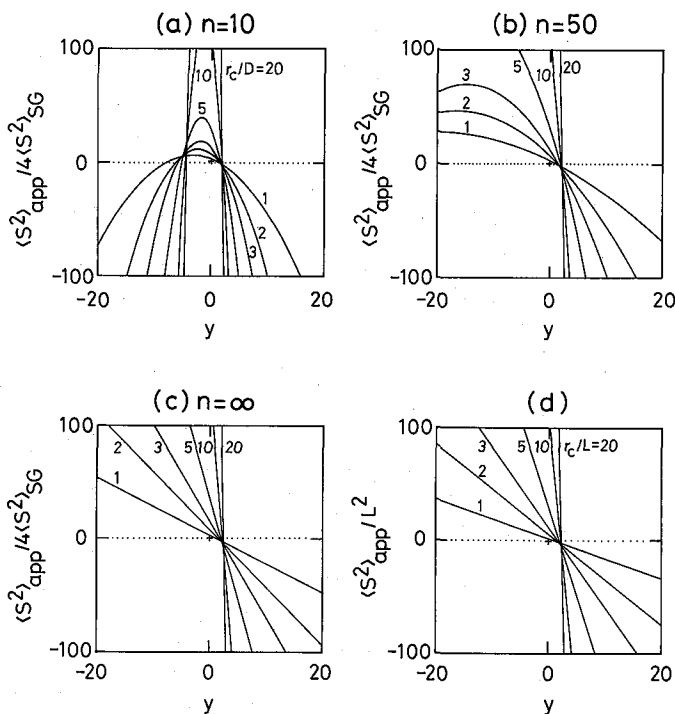


Figure 6. Variation of the reduced apparent mean-square radius of gyration for (a)-(c) the Gaussian-shell micelles and for (d) the rodlike-shell micelles. The parameter r_c/D or r_c/L is changed from 1 to 20, discretely. The cross symbols show the values for the star types of micelles, where the core does not exist.

in a quadratic form of y and its maximum peak position is in the negative y region. Thus, $\langle S^2 \rangle_{\text{app}}$ at $y \leq 0$ increases first and then decreases down to negative values as y increases (subfigures (a) and (b)). This tendency diminishes with increase of n and $\langle S^2 \rangle_{\text{app}}$ becomes a linear function of y at $n \rightarrow \infty$: it is always positive at negative y (subfigure (c)). The last behavior resembles well that of the rodlike-shell micelles which is shown in subfigure (d). The cross symbols in the figures at $y=0$ represent the values for the Gaussian star and rodlike star molecules, $[\langle S^2 \rangle_{\text{app}} / \langle S^2 \rangle_{\text{SG}}]_{y=0, r_c/D=0} = 3 - 2/n$ and $[\langle S^2 \rangle_{\text{app}} / L^2]_{y=0, r_c/L=0} = 1/3$, respectively.^{9,10}

ANALYSIS OF EXPERIMENTAL DATA

The experimental data of the particle scattering function for the ionic-non-ionic diblock copolymer in aqueous solution have been obtained by us⁴ measuring extremely dilute salt-free aqueous solution of poly(N-ethyl-2-vinylpyridinium hydroxide)-*block*-polystyrene (PVPQ-PS) at 25°C. The molecular weight of the sample was 2.42×10^5 , the molecular weights of the subchains being $M_{\text{PS}} = 1.02 \times 10^5$ and $M_{\text{PVPQ}} = 1.40 \times 10^5$. A He-Ne laser was used as the light source. In the present polymer/solvent system, the polymer was found to associate and to form micelles composed of PS-core and

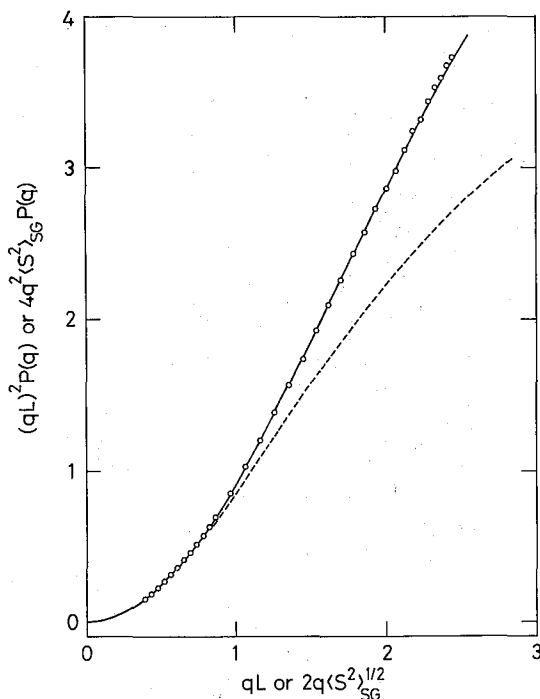


Figure 7. The results of the data fitting. The unfilled circles represent the data for poly(N-ethyl-2-vinylpyridinium hydroxide)-*block*-polystyrene in salt-free aqueous solution at 25°C. The solid line denotes the theoretical $P(q)$ calculated for the rodlike-shell micelles with $r_c = 10.7$ nm and $L = 95.7$ nm, while the broken line for the Gaussian-shell micelles with the same values, $r_c = 10.7$ nm and $D = 2\langle S^2 \rangle_{\text{SG}}^{1/2} = 95.7$ nm.

PVPQ-shell. The association number n was about 30 and the root-ms radius of gyration $\langle S^2 \rangle_{\text{app}}^{1/2}$ was 50 nm.

With the values that $\nu_{\text{PS}}=0.26$, $\nu_{\text{PVPQ}}=0.27$, $n_0=1.33125$ for $\lambda_0=633$ nm at 25°C , $w_{\text{PS}}=0.42$ and $w_{\text{PVPQ}}=0.58$, we can examine the structure of the PVPQ-PS micelles by fitting the data to the $P(q)$ curves calculated in the previous sections. Since we can set that $n=32$ and $y=0.41$, the data fitting can be pursued by using $r_c/L(D)$ and r_c as adjustable parameters.¹¹ Figure 7 shows the results, where the Kratky plot is adopted. The solid curve represents the theoretical curve for the rodlike-shell micelles with $r_c=10.7$ nm and $L=95.7$ nm ($r_c/L=0.11$), and the broken curve represents that for the Gaussian-shell micelles with the same parameters. The data points are found to be reproduced completely by the former curve. The value $L=95.7$ nm corresponds to 40% of the fully stretched length of the PVPQ subchain, ca. 240 nm. This indicates that the PVPQ chains in the shell are fairly stretched in aqueous solution due to the electrostatic repulsion between positive charges of N-ethyl-2-vinylpyridinium residues.

If we use the same procedure, we might be able to explain the data by the Gaussian-shell model with different molecular parameters because the experimental $qL(D)$ region is not so large. The results is that $r_c=10.7$ nm and $\langle S^2 \rangle_{\text{SG}}^{1/2}=D/2=32.8$ nm ($r_c/D=0.163$). However, this D value obtained is too large for the Gaussian chain with given M_{PVPQ} : it is about 3 times larger than the size of the fully swollen PS chain which has the same molecular weight as the PVPQ precursor.

Acknowledgment. We are grateful to Dr. T. Fukuda for helpful discussions on the Gaussian-shell model.

References and Notes

- (1) Tanaka, T.; Kotaka, T.; Inagaki, H. *Polymer J.* 1972, 3, 327; *Bull. Inst. Chem. Res., Kyoto Univ.* 1977, 55, 206.
- (2) Tanaka, T.; Kotaka, T.; Hattori, M.; Inagaki, H. *Macromolecules* 1978, 11, 138.
- (3) Hirata, M.; Tsunashima, Y. *Macromolecules* 1989, 22, 249. Inconsistence with the issue data is due to the fact that the nominal data of this Bulletin is 1988, 66, No. 3 and the real date is March, 1989.
- (4) Hirata, M. Doctoral Thesis, Kyoto Univ., 1988. Hirata, M.; Nemoto, N.; Tsunashima, Y.; Kurata, M. In "Ordering and Organization in ionic Solution"; Ise, N.; Sogami, I., Ed.; World Scientific: Singapore, 1988.
- (5) Benoit, H.; Frolich, D. In "Light Scattering from Polymer Solutions"; Huglin, H. B., Ed.; Academic Press: London, 1972.
- (6) Burchard, W. *Adv. Polymer Sci.* 1983, 48, 1.
- (7) Rayleigh, J. W. *Proc. Roy. Soc.* 1941, A90, 219.
- (8) Debye, P. *J. Appl. Phys.* 1944, 15, 338.
- (9) Benoit, H. *J. Polym. Sci.* 1953, 11, 507.
- (10) Burchard, M. *Macromolecules* 1974, 7, 841.
- (11) If the PS core has the same density as in the bulk state ($d_c=1.05$ gcm⁻³), the core radius of n pieces of PS molecules can be estimated as

$$r_c = [(nM_{\text{PS}}/N_A d_c)/(4\pi/3)]^{1/3} = 0.145(nM_{\text{PS}})^{1/3} \text{ (nm)}$$

Based on this r_c value and $\langle S^2 \rangle_{\text{app}}^{1/2}=50$ nm (experimental data), we can approximately evaluate L or $\langle S^2 \rangle_{\text{SG}}$ by using eq 8 or 11.

Self Diffusion of Block Copolymers in Solution.

Tadashi INOUE**, Norio NEMOTO, and Michio KURATA*

Received September 28, 1988

The self diffusion coefficient of solutions of styrene-ethylene/butylene-styrene triblock copolymer (SEBS) in a mixed solvent of tetradecane and dibutyl phthalate was measured using forced Rayleigh scattering technique. The measurements were made in the range of temperature T from 20°C to 110°C and of concentration C from 5 wt% to 30 wt% where the order-disorder transition was included. The diffusion mechanism of SEBS in the disordered state was found to be different from that of homopolymer system. The enthalpic interaction between the unlike segments affects the diffusion behavior. In the region which is slightly below the order-disorder transition region, we found that self diffusion behavior of SEBS could not be described by single self diffusion coefficient D_s . In the ordered state, SEBS is found to form micelles on the regular lattice structure from small angle X-ray scattering measurements. We have found that SEBS can diffuse in the lattice structure. This suggests that the lattice structure is not permanent, but in the dynamical equilibrium. We have also found that in the ordered state, there are two diffusion modes. The slower diffusion mode is the diffusion of SEBS micelles which forms lattice. However, the faster diffusion mode is not characterized.

KEY WORDS: Self Diffusion/ Block Copolymer/ Microdomain Structure/

INTRODUCTION

One of the most important properties of block copolymers is that they undergo the microphase separation characteristic of spatially periodical coexisting phases^{1,2}. The connectivity of the blocks prevents the macroscopic phase separation observed in homopolymer blends. The equilibrium aspect of microdomain structures has been studied experimentally or theoretically in recent years³⁻⁵. The enthalpic interaction between statistical segments of types A and B, which is often described by the dimensionless Flory parameter, χ , plays an important role in determining the equilibrium thermodynamic state of A-B diblock or A-B-A triblock copolymer. The enthalpic interaction between the unlike segments may also affect the diffusive motion of block copolymer. However, there is neither theoretical prediction nor experimental data about the Brownian motion of block copolymers.

In this report, we discuss the diffusion mechanism of a block copolymer in the ordered and the disordered states. The self diffusion coefficient (D_s) of the block copolymer in solution is measured by using forced Rayleigh scattering (FRS) technique in the wide range of temperature and concentration where the order-disorder transition point is included. The FRS technique needs labeling of polymers with a suitable phototropic dye. Typical block copolymers such as styrene-isoprene copolymer or styrene-butadiene copolymer have C-C double bonds, so that the labeling of them is

* 井上正志, 根本紀夫, 倉田道夫: Laboratory of Fundamental Material Properties, Institute for Chemical Research, Kyoto University, Uji, Kyoto 611.

** Present Address: Department of Polymer Chemistry, Faculty of Engineering, Kyoto University, Sakyo-ku, Kyoto 606.